

Proceedings Article

MPI visualization and inductive heating of hybrid implant fibers

B. Mues¹ · B. Tired² · B. Bauer³ · J. Ortega³ · T. Gries³ · T. Schmitz-Rode¹ · P. Goodwill² · I. Slabu^{1,*}

¹Applied Medical Engineering, Helmholtz Institute, RWTH Aachen University, Germany

²Magnetic Insight, Inc., Alameda, CA, USA

³Institut für Textiltechnik, RWTH Aachen University, Germany

*Corresponding author, email: slabu@ame.rwth-aachen.de

© 2020 Mues *et al.*; licensee Infinite Science Publishing GmbH

This is an Open Access article distributed under the terms of the Creative Commons Attribution License (<http://creativecommons.org/licenses/by/4.0>), which permits unrestricted use, distribution, and reproduction in any medium, provided the original work is properly cited.

Abstract

In this study, we evaluate the hyperthermia efficiency of polypropylene (PP) fibers with incorporated magnetic nanoparticles (MNP), which are used to develop inductive heatable stents in cancer therapy. Further, we investigate their depiction in magnetic particle imaging (MPI). We show that the intrinsic loss power (ILP) value depends on the MNP agglomeration state and their concentration inside the fibers, while the intensity values in the MPI images show a linear response with MNP concentration. We conclude that MNP dynamic magnetic behavior strongly changes with different MNP agglomeration states and magnetic field settings.

I Introduction

Patients with endoluminal tumors (e.g. trachea carcinoma, esophagus adenocarcinoma or bile duct Klatskin tumors), are treated by implantation of metallic stents to widen the occluded endoluminal site. However, after a while tumor tissue ingrowth takes place causing a reclosure, so-called restenosis, of the endoluminal organs. The application of a hybrid stent made of fibers with incorporated magnetic nanoparticles (MNP) allows performing local hyperthermia treatment and, in this way, destroying the tumor tissue in close vicinity to the stent. Apoptosis of tumor cells occurs at temperatures of about 43 °C, for which healthy tissue remains unharmed [1]. Treatment of cancer cells with metallic stents heated in an alternating magnetic field (AMF) induced cell necrosis, which is usually not favored because of its higher risks of developing inflammation and damage of healthy cells. Further, metallic stents lack the ability of control-

ling the saturation temperature and showed too small energy uptake [2].

In this study, we investigate the effects of MNP incorporation inside polypropylene (PP) fibers on magnetic heating by analyzing their intrinsic loss power. These PP fibers are used for the production of hybrid stents. Further, we investigate their imaging characteristics with magnetic particle imaging (MPI, MOMENTUM™ scanner, Magnetic insight, CA, USA).

II Material and methods

Two different PP fibers were produced by melt spinning of PP pellets mixed with 3 wt% resp. 7 wt% freeze-dried MNP (PP@3%MNP resp. PP@7%MNP). The MNP had a core diameter of (10.2 ± 2.4) nm and a saturation magnetization of (99.4 ± 0.8) Am²/kg(Fe). The MNP synthesis and further characteristics are described in [3]. The exact MNP concentration inside the fibers was investigated by thermogravimetric analysis (TGA).

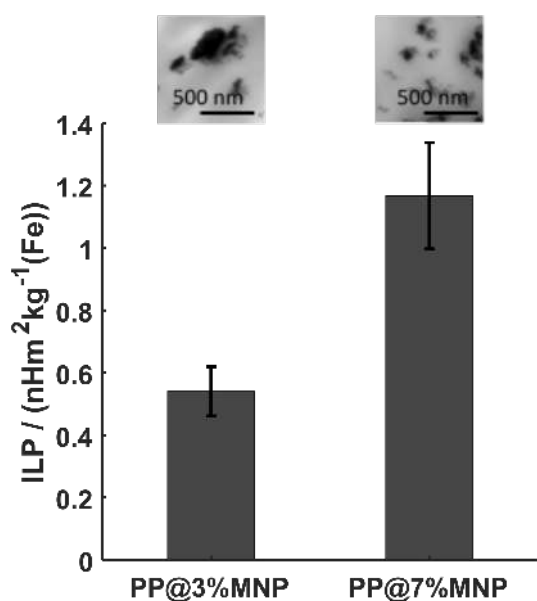


Figure 1: Intrinsic loss power (ILP) values and exemplary TEM images of PP@3%MNP and PP@7%MNP.

The PP fibers were embedded in agarose gels (1.5 wt% agarose) and exposed to an AMF at $H = 16$ kA/m and $f = 95$ kHz for 30 min. The measurements were carried out with a custom-built hyperthermia setup (Trumpf Hüttinger, Freiburg, Germany). The intrinsic loss power (ILP) value was calculated with:

$$ILP = \frac{1}{H^2 \cdot f} \cdot \frac{c}{\rho} \cdot \left. \frac{dT}{dt} \right|_{t \rightarrow 0} \quad (1)$$

where $c = 4.187$ J g⁻¹ K⁻¹ is the specific heat capacity of water, ρ the MNP weight fraction, T the temperature and t the measurement time. The magnetic field settings were chosen to achieve the best match between field parameters and particle properties (aiming at the highest expected ILP value [4]) and took medical safety limits into account ($H \cdot f \approx 1520$ kHz·kA/m).

For MPI measurements, the fibers were coiled around 15 mL sample tubes. MPI measurements were performed with a MOMENTUM™ scanner (Magnetic insight, CA, USA). Each sample was scanned in 2D projection mode, using high-resolution settings (Gradient 6.1 T/m, RF excitation amplitude = 22 mT). Rectangular ROI of similar size were placed over a linear section of each image to quantitate the relative amount of signal.

III Results and discussion

TGA measurements yield an iron MNP concentration of (2.7 ± 0.2) wt% and (7.2 ± 0.2) wt% for the samples PP@3%MNP and PP@7%MNP, respectively. Figure 1 shows the ILP values for both fibers. The ILP is approxi-

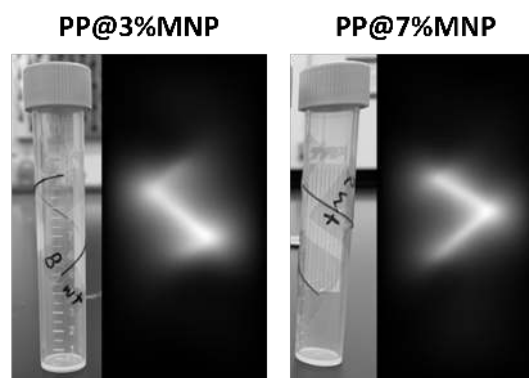


Figure 2: Photo of PP fibers with the corresponding MPI projection images for PP@3%MNP and PP@7%MNP fibers with a thickness of approx. 500 μm.

mately 53 % higher for the fibers with 7 wt% MNP compared to the ones with 3 wt% MNP. By transmission electron microscopy images, bigger MNP agglomerates could be evidenced for the PP@3%MNP than for the PP@7%MNP (see Figure 1).

Figure 2 shows a photo and the corresponding MPI 2D projection image of the PP fibers for PP@3%MNP (left image) and PP@7%MNP (right image). Both fibers with a thickness of approximately 500 μm are clearly delineated and no difference in resolution is observed between the two different concentrations. The mean signal for the PP@7%MNP fiber was 2.7 times the respective value of the PP@3%MNP fiber.

The hyperthermia measurements show a significant increase in magnetic heating (ILP) for the sample with higher amount of MNP. Such an increase in ILP could be explained by smaller agglomerations formed in the fiber with higher amount of MNP. For MNP agglomerates, the dipolar particle-particle interaction and the effective anisotropy energy increase, directly influencing the non-linear dynamic magnetic susceptibility of the MNP. Since hyperthermia and MPI rely on the non-linear dynamic magnetic susceptibility, the same behavior is expected for both techniques [5]. For the MPI images, however, a linear intensity increase with MNP concentration and visually no difference in resolution for different MNP concentrations are observed. To explain this, the effects on MNP relaxation at different magnetic field settings in dependence of MNP agglomerate size and concentration must be further investigated and the measurements will be complemented with other techniques, e.g. with AC-susceptibility measurements.

IV Conclusions

In this study, the MPI visualization and hyperthermia performance of hybrid implant fibers were investigated with

respect to MNP concentration and agglomeration formation. The results show that the ILP values are smaller for lower concentration and bigger agglomerates. High-resolution 2D projection MPI images indicate a linear intensity dependence on MNP concentration. Further measurements are planned to validate the results.

Acknowledgments

The research project is funded as part of the program “Joint Industrial Research (IGF)” of the German Federal Ministry of Economic Affairs and Energy (contract number: 19735 N).

Author’s Statement

B. Tired and P. Goodwill are full-time employees for Magnetic Insight, CA, USA. The other authors state no con-

flict of interest. Informed consent was obtained from all individuals included in this study.

References

- [1] K. F. Chu, Thermal ablation of tumours: biological mechanisms and advances in therapy, *Nat. Rev. Cancer*, vol. 14, 2014, pp. 199-208.
- [2] M.G. Floren, Noninvasive Inductive Stent Heating: Alternative Approach to Prevent In-stent Restenosis?, *Invest. Radiol*, vol. 39, 2004, pp. 264–270.
- [3] B. Mues, Towards optimized MRI contrast agents for implant engineering: Clustering and immobilization effects of magnetic nanoparticles, *J. Magn. Magn. Mater*, vol. 471, 2019, pp. 432-438.
- [4] U. M. Engelmann, Predicting size-dependent heating efficiency of magnetic nanoparticles from experiment and stochastic Néel-Brown Langevin simulation, *J. Magn. Magn. Mater*, vol. 471, 2019, pp. 450-456.
- [5] K. M. Krishnan, Biomedical Nanomagnetism: A Spin Through Possibilities in Imaging, Diagnostics, and Therapy, *IEEE Trans. Magn*, vol. 46, 2010, pp. 2523-2558.